International Journal of Engineering, Mathematical and Physical Sciences
ISSN: 2517-9934
Vol:6, No:7, 2012

Simulation of the Temperature and Heat Gain by Solar Parabolic Trough Collector in Algeria

M. Ouagued, A. Khellaf

***Abstract*—**The objectif of the present work is to determinate the potential of the solar parabolic trough collector (PTC) for use in the design of a solar thermal power plant in Algeria. The study is based on a mathematical modeling of the PTC. Heat balance has been established respectively on the heat transfer fluid (HTF), the absorber tube and the glass envelop using the principle of energy conservation at each surface of the HCE cross-sectionn. The modified Euler method is used to solve the obtained differential equations. At first the results for typical days of two seasons the thermal behavior of the HTF, the absorber and the envelope are obtained. Then to determine the thermal performances of the heat transfer fluid, different oils are considered and their temperature and heat gain evolutions compared.

***Keywords*—**Direct solar irradiance, solar radiation in Algeria, solar parabolic trough collector, heat balance, thermal oil performance

I. Introduction

THE territory of the Large Algerian Sahara (GSA), an arid and semi arid region, accounts for more than 90% of the total surface area of the country (2 381,754 km^2). The sunshine duration on almost the near total of the territory exceeds 2500 hours per year and can reach up to 3900 hours per year in the High plains and the Sahara. Indeed, exceptional opportunities arise all over the area to exploit the huge solar energy potentiality of the Sahara. From these, came the idea to carry out this work on a tracking Solar Parabolic Trough Collector (PTC). The aim is to determine the performance of these systems under the Algerian conditions, taking into account the harsh climatic conditions specific to the area. By exploiting the direct solar radiation, considered as the principal resource, these technologies offer a real alternative to the fossil resources with a little or no environmental impact and a strong potential of cost cutting as well as the possibility of hybridization of these installations [1], [2]. In order to deliver high temperatures with good efficiency, a high performance solar collector is required. Systems with light structures and low cost technology for process heat application up to 500 °C could be obtained with Solar Parabolic Trough Collector (solar PTC) [3], [4].

II. Energy Balance Model Of The Parabolic Trough Collector Review Stage

The HCE consist of an absorber inside a glass envelope. The absorber is a stainless steel tube about 70 mm in diameter with a special coating (selective coating) on the outside surface to provide the required optical properties.

M. Ouagued is with the Departement of Enegeering Process, UHBC Chlef University, PB 151-02000 Chlef, Algeria (phone: 213-774-506980; fax: 213-2772-1794; e-mail: ouagued_malika@ yahoo.fr).

A. Khellaf is with the Renewable Energies Development Center , CDER, Algiers, BP-62 Bouzereah, Algiers, Algeria (e-mail: khellaf@hotmail.com).

The selective coating has a high absorptance for radiation in the solar energy spectrum, and low emittance in the long wave energy spectrum to reduce thermal radiation losses [5]. The glass envelope protects the absorber from degradation and reduces heat losses. It is made from Pyrex, which maintains good strength and transmittance under high temperatures. The annulus space between the absorber and the glass envelop is under vacuum to reduce thermal losses and protect the selective coating [6]. The following assumptions have been made in the mathematical model:

1) The solar PTC has two tracking system that perfectly follows the sun during the day.
2) One dimensional flow.
3) Constant diameters and concentrator surfaces
4) Negligible conduction losses at the ends of each trough.

The HCE performance model uses an energy balance between the HTF and the atmosphere, and includes all equations and correlations necessary to predict the terms in the energy balance, which depend on the collector type, HCE condition, optical properties, and ambient conditions. Fig.1 presents the heat transfer plant for the parabolic through collector [5]-[7].

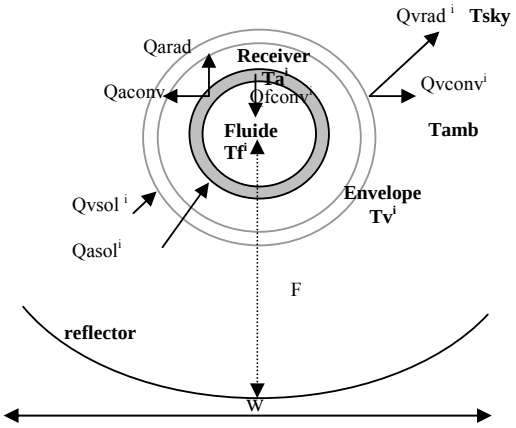

Fig. 1 Heat transfer plant for a solar PTC

A. Energy balance on the HTF

We start with a heat balance of the heat transfer fluid HTF that comes down to a partial equation of temperature, the distance along the receiver tube is indicated by "z" [5]-[8]. Therefore the equation of the HTF during the time t in a segment "i" of Δz length to the z position is given by:

$$mf^i.Cf.\frac{dTf^i}{dt} = Qz - Q(z+\Delta z) + Qfconv^i ; (i = 1, N) \qquad (1)$$

Where
Qz : heat rate coming to the segment 'i' length Δz, (W)
Qz+Δz : heat rate leaving from the segment 'i', (W)
$Qfconv^i$ *:* convection heat transfer rate between the heat transfer fluid and wall of the absorber pipe in the segment 'i', (W)

Heat balance per unit of segment length is:

$$\rho f.Af.Cf.\frac{dTf^i}{dt} = \begin{bmatrix} \text{Ff.}\rho\text{f.}\frac{\text{Cf}(\text{Tf}^{i-1}-\text{Tf}^i)}{\Delta z} + \\ \text{hf.}\pi.\text{Dai}(\text{Ta}^i - \text{Tf}^i) \end{bmatrix} \quad (2)$$

With:

$$Af = \pi Dai^2/4 \quad (3)$$

B. Energy balance on the receiver

By the analogy with the equation of the HTF, the equation of the tube receiver in every segment i is given [5]-[10]:

$$ma^i.Ca.\frac{dTa^i}{dt} = Qasol - Qfconv^i - Qaconv^i - Qarad^i \quad (4)$$
$$(i = 1, N)$$

Where:
Q_{asol} *:* incident solar irradiation absorption rate into the receiver segment "i", (W)
$Qaconv^i$ *:* convection heat transfer rate for receiver segment "i" between the surface of the absorber pipe to the surface of the glass envelope, (W)
$Qarad^i$: radiation heat transfer rate for receiver segment "i" between the surface of the absorber pipe to the surface of the glass envelope, (W)

Heat balance per unit of segment length is:

$$\rho a\ .Aa\ .Ca\ \frac{dTa^{\ i}}{dt} = \begin{bmatrix} Qsol\ .\eta_a.\alpha_a - \\ hf\ .\pi\ .Dai\ .\left(Ta^{\ i} - Tf^{\ i}\right) - \\ ha\ .\pi\ .Dae\ .\left(Ta^{\ i} - Tv^{\ i}\right) - \\ \frac{\sigma\ .\pi\ .Dae\ .\left(Ta^{\ i\,4} - Tv^{\ i\,4}\right)}{\frac{1}{\varepsilon_a} + \frac{(1-\varepsilon_v).Dae}{\varepsilon_v.Dvi}} \end{bmatrix} \quad (5)$$

With

$$Aa\ = \frac{\pi}{4}\left(Dae^{\ 2} - Dai^{\ 2}\right) \quad (6)$$

$$Qsol\ = Iba\ .\frac{A}{L} \quad (7)$$

$$A = w.L \quad (8)$$

$$\eta_a = \eta_v.\tau_v \quad (9)$$

$$\eta_v = \varepsilon_1.\varepsilon_2.\varepsilon_3.\varepsilon_4.\varepsilon_5.\varepsilon_6.\rho_{cl}.k \quad (10)$$

$$k\ = \cos\theta_i + 0{,}000884\ .\theta_i - 0{,}00005369\ .\theta_i^2 \quad (11)$$

Where:
ε_1*:* HCE shadowing (bellows, shielding, supports)
ε_2*:* tracking error
ε_3: geometry error (mirror alignment)
ε_4: dirt on mirror
ε_5: dirt on HCE
ρ_{cl}: clean mirror reflectance
k: incident angle modifier.
θi*:* incident angle, (deg)

C. Energy balance on the glass envelope

By analogy with the equation of the receiver and the HTF, the equation of the glass envelope in every segment " i " is given [5]-[11]:

$$mv^{\ i}.Cv.\frac{dTv^{\ i}}{dt} = \begin{bmatrix} Qvsol^{\ i} + Qarad^{\ i} + \\ Qaconv^{\ i} - \\ Qvrad^{\ i} - Qvconv^{\ i} \end{bmatrix}; (i = 1, N) \quad (12)$$

Where:
$Qvsol^i$: incident solar irradiation absorption rate into the glass envelope of receiver segment "i", (W)
$Qvrad^i$: radiation heat transfer rate between the outer surface of the glass envelope to the sky receiver segment "i", (W)
$Qvconc^i$: convection heat transfer rate between the surface of the glass envelope to the atmosphere for receiver segment "i", (W)

Heat balance per unit of segment length is:

$$\rho_v\ .Av\ .Cv\ .\frac{dTv^{\ i}}{dt} = \begin{bmatrix} Qsol\ .\eta_v.\alpha_v + \\ ha\ .\pi\ .Dae\ .\left(Ta^{\ i} - Tv^{\ i}\right) + \\ \frac{\sigma\ .\pi\ .Dae\ .\left(Ta^{\ i\,4} - Tv^{\ i\,4}\right)}{\frac{1}{\varepsilon_a} + \frac{(1-\varepsilon_v).Dae}{\varepsilon_v.Dvi}} - \\ hv\ .\pi\ .Dve\ .\left(Tv^{\ i} - Tamb\ \right) - \\ \sigma\ .\pi\ .Dve\ .\varepsilon_v.\left(Tv^{\ i\,4} - Tsky^{\ 4}\right) \end{bmatrix} \quad (13)$$

With

$$Av\ = \frac{\pi}{4}.\left(Dve^{\ 2} - Dvi^{\ 2}\right) \quad (14)$$

$$Tsky = 0{,}0552.Tamb^{1{,}5} \quad (15)$$

The total Heat gain per unit length of the receiver (W/m) is:

$$Qgain = \sum_1^N (\text{Qfconv}^i.\Delta Z)/L \quad (16)$$

The total daily heat gain (J/m/day) is:

$$Qgainday\ \ = h.\sum_{i=1}^{S_0-1} \text{Qgain}_{\ 1+\text{ih}} \quad (17)$$

III. Convection Heat Transfer Coefficients

A. HTF convection heat transfer (hf)

The HTF convection heat transfer coefficient is:

$$hf = Nuf \cdot \frac{kf}{Dai} \quad (18)$$

Where
Nu_f : Nuselt number at Tf,
kf : thermal conductance of the HTF at Tf, (W/m.K)

The Nusselt number depends on the type of flow through the HCE. At typical operating conditions, the flow is well within the turbulent region. However, during off-solar hours, the flow may become transitional or laminar because of the viscosity of the HTF at lower temperatures. Therefore, the Nusselt number for each flow condition is:

1. Turbulent and transitional flow cases ($2300 \le Re \le 5.10^6$ et $0,5 \le Pr \le 2000$)

To estimate the convective heat transfer from absorber to the HTF for these cases, the following number correlation developed by Gnielinski (1976) [9]-[12] is used.

$$Nu_f = \frac{\left(f/8\right).\left(\mathrm{Re}-1000\right).\mathrm{Pr}}{1+12,7.\sqrt{f/8}\left(\mathrm{Pr}^{2/3}-1\right)} \quad (19)$$

With

$$f = \left(0,79.\log_{10}\left(\mathrm{Re}\right)-1,64\right)^{-2} \quad (20)$$

$$\mathrm{Re}_f = \frac{\rho_f.v_f.Dai}{\mu_f} \quad (21)$$

$$\mathrm{Pr}_f = \frac{Cf.\mu_f}{k_f} \quad (22)$$

$$v_f = \frac{4.Ff}{\pi.Dai^2} \quad (23)$$

Where
f: friction factor for the inner surface of the inner surface of the absorber pipe
Re_f : Reynolds number at Tf;
Pr_f : Prandtl number at Tf;
v_f: HTF rate, (m/s) ;
μ_f : Dynamic viscosity of the HTF, (kg/m.s) ;

All the fluid properties (c_f, k_f, μ_f, ρ_f) are evaluated at Tf. The correlation (41) assumes uniform heat flux and temperature, and assumes the absorber has a smooth inner surface.

2. Laminar flow case (Re < 2300)

When the laminar option is chosen and the Reynolds number is lower than 2300, the Nusselt number will be constant. For pipe flow, the value will be 4,36 [11].

B. Convection heat transfer cofficient for the annulas gas (ha)

Two heat transfer mechanisms are used to determine the convection heat transfer coefficient between the absorber and the glass envelop: the free-molecular convection and the natural convection (KJCOC 1993) [13].

1. Free-molecular convection (Pa≤100 mmHg)

When the HCE annulus is under vaccum (Pa ≤ 100 mmhg), the convection heat transfer between the a bsorber ans glass envelope occurs by free-molecular convection (Ratzel et al ,1979) [11].

$$ha = \frac{kstd}{\left(\frac{Dae}{2.Ln\left(Dvi/Dae\right)}+b.\lambda.\left(\frac{Dae}{Dvi}+1\right)\right)} \quad (24)$$

With

$$\lambda = \frac{2,331.10^{-20}.Tmoy\ 1}{Pa.\delta^2} \quad (25)$$

$$b = \frac{\left(2-a\right).\left(9.\gamma-5\right)}{2a.\left(\gamma+1\right)} \quad (26)$$

Where
$kstd$: thermal conductance, (W/m.K);
b: interaction coefficient;
λ : mean-free-path between collisions of a molecule, (cm);
δ : molecular diameter of annulus gas, (cm)
a : accommodation coefficient
γ : ratio of specific heats for the annulus
T_{moy1}: *Average* temperature, ($T_{moy1}=(Ta+Tv)/2$), (K)

2. Natural convection (Pa>100 mmHg)

When the HCE annulus loses vaccum (Pa>100mmHg), the convection heat transfer mechanism between the absorber and glass envelope occurs by natural convection. Incropera and De Witt (1990) correlation for natural convection in an annular space between horizontal cylinders is used for this case [11].

$$ha = \frac{2.keff}{Dae.Ln\left(Dvi/Dae\right)} \quad (27)$$

With

$$\frac{keff}{ka} = 0,386.\left(\frac{\mathrm{Pr}_a}{0,861+\mathrm{Pr}_a}\right)^{1/4}.Rac^{1/4} \quad (28)$$

$$Rac = \frac{g.\beta.\left(Ta-Tv\right).Lc^3}{\upsilon_a.\alpha_a} \quad (29)$$

$$Lc = \frac{2.\left[Ln\left(Dvi/Dae\right)\right]^{4/3}}{\left[\left(\frac{Dvi}{2}\right)^{-3/5}+\left(\frac{Dae}{2}\right)^{-3/5}\right]^{5/3}} \quad (30)$$

$$\Pr_a = \frac{c_a . \mu_a}{k_a} \quad (31)$$

$$\beta_a = \frac{1}{Tmoy\,1} \quad (32)$$

Where
keff : Effectif thermal conductance of annulus gaz , (W/m.K);
k_a : thermal conductance of annulus gaz at Tmoy1, (W/m.K);
g : gravitational constant, (9,8 m^2/s);
β_a : volumetric thermal expansion coefficient (ideal gas), (K^{-1});
υ_a : kinematic viscosity of the annulus gaz, (m^2/s)
α_a : thermal diffusivity of the annulus gaz, (m^2/s)
c_a: HTF heat specific of the annulus gaz, (J/kg.K)
μ_a: Dynamic viscosity of the annulus gaz, (kg/m.s)

Correlation (28) is valid for range of $0,7 \leq Pr_a \leq 6000$ and $Rac \leq 10^7$. All physical properties (α_a, β_a, υ_a, k_a, c_a, μ_a) are evaluated at the average temperature Tmoy1.

C. Convection heat transfer coefficient for air ambient (hv)

The convection heat transfer coefficients form the glass envelope to the atmosphere:

$$hv = Nu_{air} . \frac{k_{air}}{Dve} \quad (33)$$

Where
Nu_{air} : Nuselt number at Tmoy2
k_{air} : thermal conductance of the air ambient at Tmoy2, (W/m.K)
Tmoy2: Average temperature, (Tmoy2=(Tv^i+Tamb)/2), K

The Nusselt number depends on whether the convection heat transfer is natural (no wind) or forced (with wind)

1. No wind case (natural convection)

For this case, the correlation developed by Churchill et Chu (1990) will be used to estimate the Nusselt number [11], [14].

$$Nu_{air} = \left[0,6 + \frac{0,387 . Ra^{1/6}}{\left[1 + (0,559 / \Pr)^{9/16}\right]^{8/27}} \right]^2 \quad (34)$$

With

$$Ra = \frac{g . \beta_{air} . (Tv - Tamb) . Dve^3}{\alpha_{air} . \upsilon_{air}} \quad (35)$$

$$\beta_{air} = \frac{1}{Tmoy\,2} \quad (36)$$

$$\Pr_{air} = \frac{\upsilon_{air}}{\alpha_{air}} \quad (37)$$

Where
β_{air} *:* volumetric thermal expansion coefficient (ideal gas), (K^{-1})
α_{air} : thermal diffusivity for the air at Tmoy2, (m^2/s)
υ_{air} : kinematic viscosity for the air at Tmoy2, (m^2/s)

Correlation (34) is valid for the $10^5 \leq Ra \leq 10^{12}$. All fluid properties are assumed at Tmoy2.

2. Wind case (forced convection)

If there is wind, the convection heat transfer will be forced convection. The correlation developed by Zhukauskas will be used to estimate the Nuselt number [11].

$$Nu_{air} = C . \mathrm{Re}_{air}^{\,m} . \Pr_{air}^{\,'n} . \left(\frac{\Pr_{air}^{'}}{\Pr_{air}^{''}} \right)^{1/4} \quad (38)$$

With

$$\mathrm{Re}_{air} = \frac{\rho_{air} . v_{air} . Dve}{\mu_{air}} \quad (39)$$

$$\Pr_{air} = \frac{c_{air} . \mu_{air}}{k_{air}} \quad (40)$$

TABLE I
PARAMETERS OF THE CORRELATION (38)

Re	C	m
1-40	0,75	0,4
40-1000	0,51	0,5
1000-200 000	0,26	0,6
200 000-1000 000	0,076	0,7
n=0,37 pour Pr≤10		
n=0,36 pour Pr>10		

Where
$\Pr_{air}$' : Prandtl number for the air at Tamb;
$\Pr_{air}$' : Prandtl number for the air at Tv^i;
ρ_{air} : density of the air at Tamb, (kg/m^3) ;
v_{air} : wind speed, (m/s)
μ_{air} : dynamic viscosity of the air at Tamb, (kg/m.s);
c_{air} : air specific heat of the air at Tamb, (J/kg.K).

Correlation (38) is valid for the $0,7 \leq Pr \leq 500$ and $1 \leq Re \leq 10^6$. All fluid properties are assumed at Tamb.

IV. ALGORITHM

- We obtain a differential equations system solved by the modified Euler method. The solution process is carried out on the basis of a global algorithm (programmed in Fortran language).
- The properties including the density (kg/m3), the specific heat (J/kg-K), the dynamic viscosity (kg/m-s), and the thermal conductance (W/m-K) has been taken at the HTF saturation pressure for different temperatures.
- The collector type choices are LS-2 (table II) with two axis tracking system with vaccum in annulus space between absorber and glass envelope (Michael Geyer and al., Symposium on Concentrating Solar Power and Chemical Energy Technologies, 2002). The LS-2 is second-generation parabolic trough collectors built by Luz International Ltd [15], [16]. The HTF choices are syltherm 800 in the first case.

TABLE 1I
SOLAR PTC SPECIFICATION USED IN THE MODEL VALIDATION [15], [16]

Receiver length	7,8 m
Collector width	5 m
Focal distance	1.84
Receiver internal diameter	0,066 m
Receiver external diameter	0,07 m
Receiver thermal conductivity	54 w/m.K
Glass cover internal diameter	0,115 m
Glass cover internal diameter	0,109 m
Concentration ratio	22,42
Receiver absorptance	0,906
Receiver emittance	0,14
Glass cover transmittance	0,95
Inclinaison angle modifier	1
Heat transfer fluid flow rate	0,001 m^3/s
Annulus pressure	0,01 mmHg
Density of the absorber selective coating	$8,02.10^3$ kg/m^3
Absorber specific heat	500 J/kg.K
Density of Pyrex glass envelope	$2,23.10^3$ kg/m^3
Glass envelope specific heat	1090 J/kg.K
HCE Shadowing	0,974
Tracking Error	0,994
Geometry Error (mirror alignment)	0,98
Reflected surface reflectivity	0,93
Clean Mirror Reflectance	0,935
Glass envelope emittance	0,86
Glass envelope absorptance	0,02

- The Ambient Conditions section includes direct normal incident solar irradiation, wind speed, ambient temperature from the select location for clear days from different seasons of the year [16], [17].

V. NUMERICAL RESULT

Simulation results of the outlet temperature of Syltherm 800, of the absorber and of the glass envelope for typical days in the daylight period in clear sky are presented in fig. 2 and fig. 4. The Syltherm 800 heat gain per unit length of receiver with fluid temperature is also presented in fig. 3 and fig. 5.

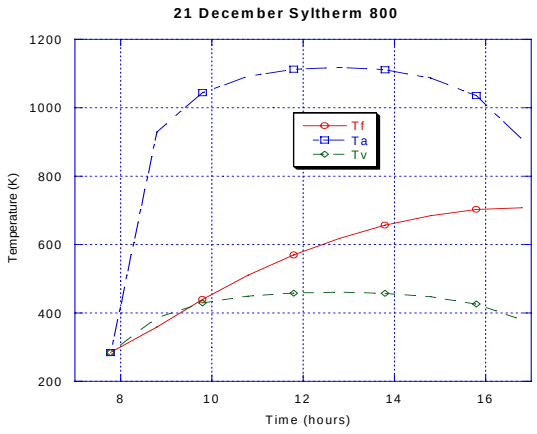

Fig. 2 Syltherm 800, absorber and glass envelope temperatures in day 21 December

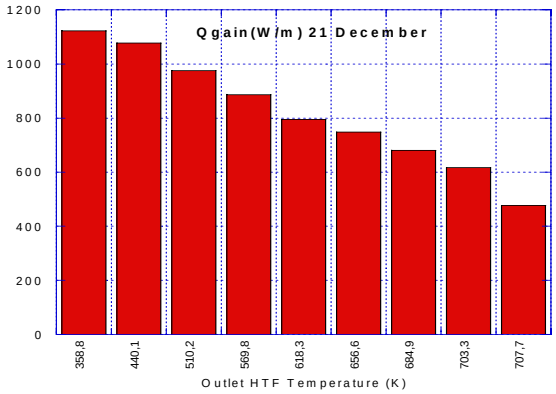

Fig. 3 Syltherm 800 Heat gain per unit length of receiver with temperature in 21 December

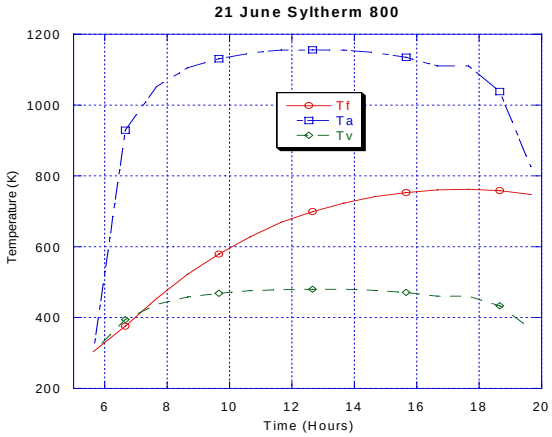

Fig. 4 Syltherm 800, absorber and glass envelope temperatures in day 21 June

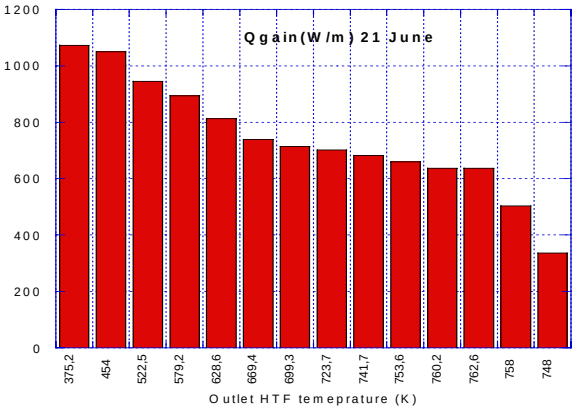

Fig. 5 Syltherm 800 Heat gain per unit length of receiver with temperature in 21 June.

Fig. 2 and fig. 4 represent the variation of the temperatures of syltherm 800, of the absorber and of the envelope function of time for typical days of the year (summer and winter). We observed that the temperature of the absorber exceeds 1100K from 8h00 to 18h00 in June and from 11h00 to 15h00 in December. In the same way, the temperature of the envelope exceeds 450 K from 8h00 to 18h00 in June and from 11h00 to 15h00 in December.

The Syltherm 800 exceeds 750K at 16h00 during June, whereas it reaches only 700K around 16h00 during December. We observe in figures 3 and 5 that the evolution heat gain is inversely proportional to the increase of fluid temperature.

In the second part of results, we present in fig. 6 the simulation of the annual monthly mean daily heat gain of the various following thermal oils : Syltherm 800, Marlotherm X, Santotherm 59, Therminol D12 and Syltherm XLT for the six Algerian locations (Algiers, Annaba, Oran, Béchar, Ghardaia and Tamanrasset). These locations correspond to different climatic regions and locations in Algeria (table III). Below we describe some of the ideas which can be observed inspection of these results.

TABLE III
LATITUDE ANGLE, LONGITUDE ANGLE, ALTITUDE FROM MEAN SEA LEVEL, AND CLIMATE TYPE FOR DIFFERENT LOCATIONS

Location	Latitude (°)	Longitude (°)	Altitude (km)	Climate type
Algiers	36,43	3,15	0,025	Mid latitude summer
Annaba	36,8	7,8	0,040	Mid latitude summer
Oran	35,38	-0,37	0,099	Mid latitude summer
Bechar	31,38	-2,15	0,806	Tropical
Ghardaia	32,48	3,66	0,500	Tropical
Tamanrasset	22,47	5,31	1,378	Tropical

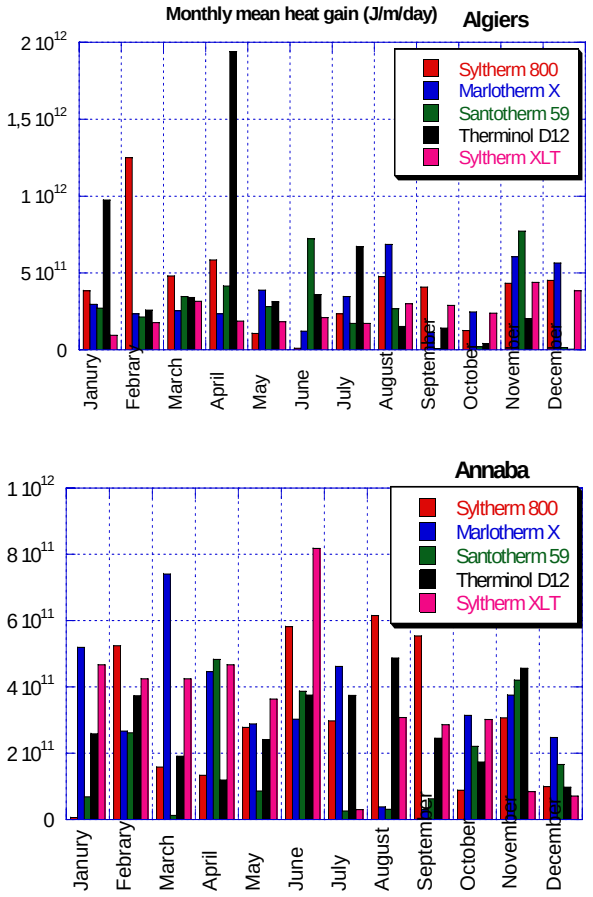

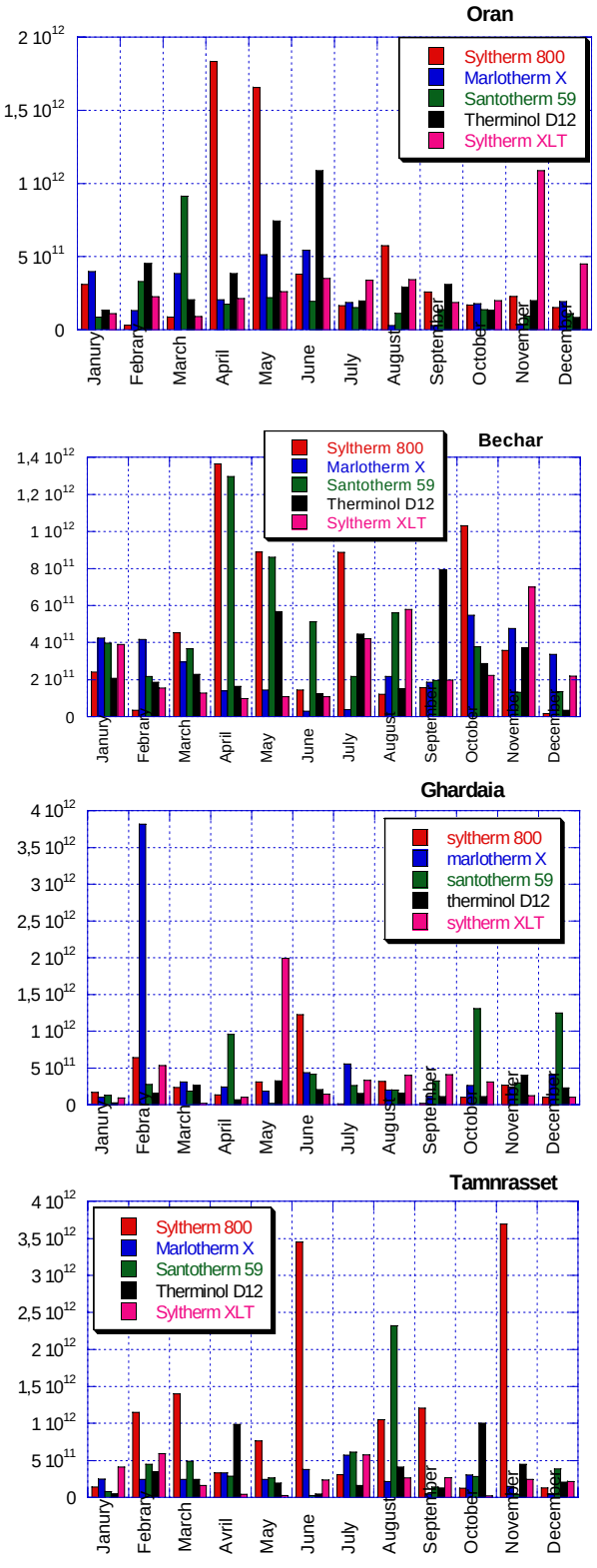

Fig. 6 Annual monthly mean daily Heat Gain of thermal oils for different locations in Algeria

We observe on the preceding figures that the monthly mean daily heat gain changes from a site to another and from a month to another at the court of year. It is also noted that for each location, some thermal oils are promoters as regards heat gain:

- In Algiers, the therminol D12 reaches 2.10^{12} J/m^2/Day on April, syltherm 800 reaches $1{,}2.10^{12}$ J/m^2/Day on Febrary and the Santotherm 59 which reaches 7.10^{11} J/m^2/Day on June and November;
- In Annaba, the Syltherm XLT reaches 8.10^{11} J/m^2/Day on June, Marlotherm X reaches 7.10^{11} J/m^2/Day on March and the Syltherm 800 reaches 6.10^{11} J/m^2/Day on June and August.
- In Oran, the Syltherm 800 reaches $1{,}8.10^{12}$ J/m^2/Day on April and May, Therminol D12 and Syltherm XLT reach $1{,}1.10^{12}$ J/m^2/Day on June and November;
- In Béchar, the Syltherm 800 reaches $1{,}4.10^{12}$ J/m^2/Day on April, the Santotherm 59 reaches $1{,}3.10^{12}$ J/m^2/Day on Avril and the Therminol D12 which reaches 8.10^{11} J/m^2/Day on September;
- In Gahrdaia, the Marlotherm X reaches $3{,}8.10^{12}$ J/m^2/Day on Febrary, the Syltherm 800 reaches 2.10^{12} J/m^2/Day on May and the Santotherm 59 which reaches $1{,}2.10^{12}$ J/m^2/Day on October and December;
- In Tamanrasset, the Syltherm 800 reaches $3{,}7.10^{12}$ J/m^2/Day on November, the Santotherm 59 reaches $2{,}2.10^{12}$ J/m^2/Day on August and the Therminol D12 which reaches 10^{12} J/m^2/Day on April and October.

VI. Conclusion

A rigorous mathematical model considering the geometrical, optical, thermal and fluid dynamic aspects of a solar PTC has been carried out. The accuracy of the detailed simulation model is demonstrated in this paper by the simulation of the change of the temperature and heat gain of the syltherm 800, change of the temperature of the absorber and the envelope during period of daylight for typical days. The second simulation was devoted to compare the increment of HTFs thermal oil temperature of solar PTC with vacuum in the space between the receiver and cover working with thermal oil. Numerical results shown that the syltherm 800 can operate at high temperature more than 700K, santotherm LT, therminol ADX10, marlotherm SH and santotherm 59 can operate between 650K and 750K and syltherm XLT and marlotherm X can operate at low temeparatue under than 700K. The simulation of the annual monthly mean heat gain per thermal oil and in the six locations selected from the Algerian territory shown that each HTF type is advantageous in a site compared to another. Also, cost and availability could dictate which HTF to use.

References

[1] A. Gama, M. Haddadi, A. Malek, " Etude et réalisation d'un concentrateur cylindro parabolique avec poursuite solaire aveugle", Revue des Energies Renouvelables Vol. 11 N°3 (2008) 437 – 451.

[2] F. Yettou,A. Malek, M. Haddadi, A. Gama, " Etude comparative de deux modèles de calcul du rayonnement solaire par ciel clair en Algérie", Revue des Energies Renouvelables Vol. 12 N°2 (2009) 331 – 346.

[3] S. A. Kalogirou, "Solar thermal collectors and applications", Prog. Energy Combust. Sci. 30 (3) (2004) 231–295.

[4] H. Price, "Guidelines for Reporting Parabolic Trough Solar Electric System Performance". NREL/CP-550-22729. Golden, CO: National Renewable Energy Laboratory (1997).

[5] J. A. Duffie, W. A. Beckman, "Solar engineering of thermal processes", 2nd ed. Madison: John Wiley &Sons, Inc., (1991).

[6] O. García-Valladares, N. Velázquez, "Numerical simulation of parabolic trough solar collector: Improvement using counter flow concentric circular heat exchangers", International Journal of Heat and Mass Transfer, (2009) 597–609.

[7] N. ESKIN, "Transient performance analysis of cylindrical parabolic concentrating collectors and comparison with experimental results ", Energy Conver, Mgnt, Vol 40, (1999) 175-191.

[8] I. Sefa, M. Demirtas, I. Olak, "Application of one-axis sun tracking system", Energy Conversion and Management 50, (2009) 2709–2718.

[9] R. Forristall, "Heat Transfer Analysis and Modeling of a Parabolic Trough Solar Receiver Implemented in Engineering Equation Solver", NREL, USA (2003).

[10] R. Siegel, J. Howell, "Thermal Radiation Heat Transfer", Fourth Edition. New York, NY: Taylor & Francis (2002).

[11] F. Incropera, D. DeWitt, "Fundamentals of Heat and Mass Transfer", sixth Edition (1990).

[12] V. Gnielinski, "New Equations for Heat and Mass Transfer in Turbulent Pipe and Channel Flow". International Chemical Engineering (16:2) (April 1976) pp. 359–363.

[13] KJC Operating Company. " Final Report on HCE Heat Transfer Analysis Code". SANDIA Contract No. AB-0227. Albuquerque, NM: Sandia National Laboratories (December 1993).

[14] S. W. Churchill, and H. H. S. Chu, "Correlating equations for laminar and turbulent free convection from a horizontal cylinder", Int. J. Heat Mass Transfer 18 (9) (1975) 1049–1053.

[15] V. E. Dudley, J. G. Kolb, A. R. Mahoney, T. R. Mancini, C. W. Matthews, Sloan and D. Kearney, " Test results: SEGS LS-2 solar collector", Report of Sandia National Laboratories (SANDIA-94-1884) (1994).

[16] Quoilin Sylvain., "Les Centrales Solaires à Concentration", Faculté des sciences appliquées, Université de Liège (2007).

[17] M. Pucara, Despicb., "The effect of diffuse/indirect light on the energy gain of solar thermal collectors", Renewable Energy 30, (2005) 1749–1758.